

# Estimation of Mercury Vapor Flux from Natural Substrate in Nevada

RICHARD E. ZEHNER\* AND  
MAE S. GUSTIN

Department of Environmental and Resource Sciences,  
University of Nevada, Reno, Nevada 89557

The contribution of mercury to the atmosphere from natural sources is not well-quantified, particularly at the regional scale. This modeling study employed a Geographic Information Systems (GIS) approach to estimate mercury flux from substrate in Nevada, which lies within one of the global belts of geologic Hg enrichment. In situ mercury flux measurements were taken from a variety of substrate types with a wide range of mercury concentrations. This empirical data forms the basis of equations applied to a database of over 71 000 rock and soil samples used in scaling mercury flux for Nevada. The GIS was employed to spatially model estimated flux values according to sample type, geology, presence/absence of hydrothermal alteration, and meteorological conditions. The area average flux calculated for Nevada adjusted for meteorological conditions is  $4.2 \pm 1.4 \text{ ng m}^{-2} \text{ h}^{-1}$ , which corresponds to a  $\sim 29 \text{ kg}$  daily emission of mercury. Areas of hydrothermal alteration emit  $12.9 \pm 3.6 \text{ ng m}^{-2} \text{ h}^{-1}$ , accounts for 22% of net mercury emissions yet represents only 7% of the area of Nevada. Unaltered geologic units have low fluxes ( $3.5 \pm 1.2 \text{ ng m}^{-2} \text{ h}^{-1}$ ) but, because of their large area, emit 78% of the total mercury.

## Introduction

Areas geologically enriched in mercury (Hg) are concentrated in, but not limited to, active plate tectonic boundaries and are associated with high crustal heat flow, volcanism, hydrothermal systems, and subsequent base and precious metal deposits (1). Naturally enriched substrates constitute long-lived sources of Hg to the atmosphere (2).

The relative contribution of Hg to the atmosphere from natural sources is currently uncertain and a topic of debate. While many anthropogenic sources represent point discharges of Hg that are relatively easy to measure, most natural sources are diffuse and difficult to characterize. Until recently, little work had been done to quantify Hg emissions from natural sources. Early estimates of Hg flux from mercuriferous belts ( $\sim 1.1 \text{ ng m}^{-2} \text{ h}^{-1}$ ) were based on the difference between emission factors for anthropogenic sources and deposition estimates (3) rather than on actual physical measurements. Recently, natural source Hg emission estimates have been made at regional and local scales based on measured fluxes and substrate Hg concentration (2, 4, 5).

This study focused on quantifying Hg emissions from natural substrate within the State of Nevada, which is an ideal locality for several reasons. It is located within one of the global Hg mineral belts, contains numerous areas of natural Hg enrichment, has excellent access, and has minimal

vegetation. Nevada has been extensively explored for mineral deposits. Because Hg analyses of substrate are often used as a geochemical exploration tool, a large database of Hg concentrations in substrate was available.

To perform the scaling, in situ derived Hg fluxes were adjusted to remove daily variability, yielding an average daily flux. The adjusted data were then used to develop an equation that allowed for estimation of average daily Hg flux, using substrate Hg concentration. This equation was applied to the database of rock and soil Hg concentrations for Nevada to estimate Hg flux. Within a Geographic Information System (GIS), these estimated flux values were used along with geologic and meteorological data to scale-up Hg emissions for the state.

This model does not address several factors known to influence mercury emissions. The effect of vegetation was not modeled, although vegetation is known to influence mercury emissions through shading and foliar exchange (6, 7). Episodic events such as rainfall and forest fires are also known to affect mercury emissions (8, 9), but the magnitude of these effects have not been quantified. In addition, several natural sources of atmospheric Hg in Nevada were not included in this study. Hg vapor has been shown to originate from deep sources not exposed at the surface (10, 11). Since this study estimated flux based on the Hg concentration of surface samples, the contribution from deep sources is not included. Similarly, the Hg flux from active geothermal systems has not been systematically measured, so estimates are not included in this model. Published estimates of the contribution from geothermal systems range from 0.3 g/day Hg at the former Sulphur Banks mercury mine (12) to 18–24 g/h from geothermal power plants (13–15).

## Natural Mercury Sources in Nevada

The mercury concentration of soils and rocks is generally low; the natural crustal average is  $0.05 \mu\text{g/g}$  (16). However, natural processes such as Hg transport and deposition in geothermal systems can elevate Hg levels in near-surface crustal rocks. In these systems, hydrothermal fluids with temperatures up to  $400 \text{ }^\circ\text{C}$  dissolve metals such as mercury and redeposit them at concentrations up to millions of times the crustal average. When exposed at the surface, these hydrothermally altered rocks can emit Hg to the atmosphere at rates of tens to 10 thousands  $\text{ng m}^{-2} \text{ h}^{-1}$  (1, 5, 8, 17).

The geology of Nevada is characterized by at least three major periods of structural deformation that faulted and fractured crustal rocks (18), forming conduits for hydrothermal fluids. The last episode involved extensional forces that thinned the crust, leading to high crustal heat flow and copious hydrothermal activity. Geothermal systems resulting from the high heat flow hydrothermally altered large volumes of rock and locally deposited or are currently depositing Hg and other metals within these altered zones. Nevada has hundreds of active hot springs and geothermal wells (19) and thousands of zones of alteration where past hydrothermal fluids flowed (Figure 1).

The same hydrothermal systems that deposit Hg also deposit other metals in economic quantities, such as gold, silver, and copper. Consequently, Nevada is one of the world's foremost gold mining regions. Many active gold mines in Nevada contain elevated Hg concentrations, and some produce Hg as a byproduct of cyanidation or smelting (20). For this reason, the Hg flux from active and recently active metal mines in Nevada was estimated.

\* Corresponding author phone: (775)784-4966; e-mail: Zehner@unr.edu.

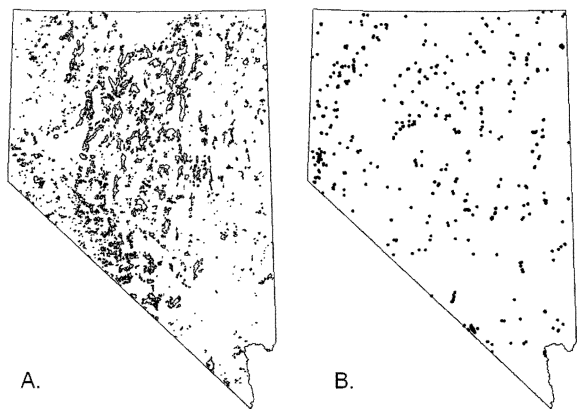


FIGURE 1. (A) Map of Nevada showing zones of hydrothermal alteration derived using LANDSAT imagery. Approximately 7% of Nevada falls within a hydrothermal alteration zone. (B) Location of present-day hot springs and geothermal wells. Data from Garside (19).

### Methods

The 303 in situ mercury flux measurements used in this study were collected using protocols outlined in refs 5 and 17. In general, Hg flux measurements utilized a cylindrical polycarbonate field flux chamber attached to a Tekran model 2537A cold vapor atomic fluorescence spectrometer on undisturbed geologic substrates. Meteorological conditions such as light intensity, substrate and air temperature, and barometric pressure were simultaneously recorded. In addition, a sample of the upper 2 cm of substrate was taken and analyzed for total Hg after aqua regia digestion by cold vapor atomic absorption spectroscopy by the Nevada Bureau of Mines and Geology.

The sample points used in the modeling consist of 71 227 rock chip, soil, mine dump, and prospect pit samples obtained from private and government agencies for projects including Hg and precious metal exploration (e.g., refs 21 and 22). These samples were analyzed for Hg by a variety of assay techniques and constitute the most comprehensive Hg data set available for Nevada. The data set consists of samples representative of unaltered rock units as well as select samples of narrow veins and alteration zones. Because sampling was not conducted on a completely random basis, the substrate sample data suffer from sample bias. The section on GIS modeling discusses how the effects of sample bias are mitigated.

**Adjustments to the Data.** The amount of Hg vapor emitted from rock and soil is strongly controlled by substrate Hg concentration, light intensity, and temperature (1, 5, 23). Because the latter two factors vary temporally over a daily cycle, it was necessary to adjust the in situ derived fluxes to be representative of an average daily flux.

Mercury flux follows a diel pattern that peaks at midday, when sun intensity is greatest (Figure 1 in Supporting Information). Because of this cycle, flux measurements taken at different times from the same location and substrate will vary. This diel pattern closely follows a Gaussian distribution, and an equation was developed (5) that allows for the normalization of Hg flux measurements taken at any time of day to an average daily flux:

$$F = C_1 \left[ \frac{1}{\sqrt{0.26\pi}} e^{-\frac{(t-0.5)^2}{2 \times 0.13^2}} \right] \quad (1)$$

where  $F$  is Hg flux (in  $\text{ng m}^{-2} \text{h}^{-1}$ ),  $C$  is a coefficient of flux magnitude, and  $t$  is time of day normalized from 0 to 1 (e.g., noon = 0.5). Equation 1 adjusts individual measurements to

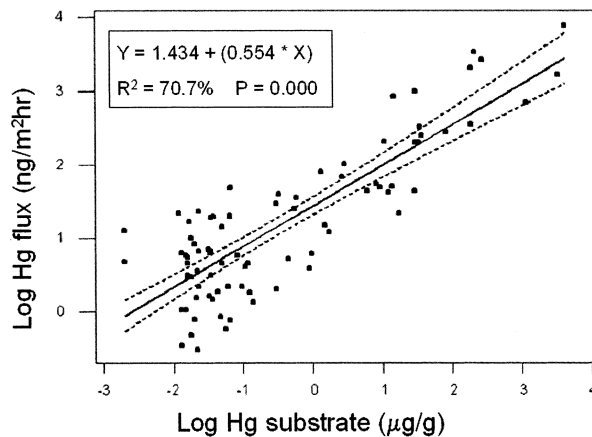


FIGURE 2. Plot of logarithm of Hg substrate versus logarithm of normalized flux for 84 samples made in direct sunlight from locations in California and Nevada. Dashed line shows 95% confidence interval. Data from geothermal sources were not included.

compensate (“normalize”) for the daily effects of solar radiation and temperature to Hg flux.

Equation 1 was derived using in situ flux data measured around the autumn equinox under average meteorological conditions from substrate with low and high concentrations (outside of the Ivanhoe mining district, Nevada; Knoxville mining district, California, respectively). Statistical tests confirm the efficacy of the equation (Table 1 in Supporting Information). The conversion transforms temporally dependant measurements to representative values useful for Hg scaling. Flux values for the remainder of this paper have been adjusted to represent average daily Hg flux.

**Derivation of Substrate–Flux Curve.** A primary factor affecting Hg flux is substrate concentration (2, 17, 24). A log–log distribution of Hg substrate concentration versus Hg flux was derived from a subset of 84 in situ flux measurements taken in direct sunlight from a variety of geologic substrates and range of Hg concentrations (0.012–4290  $\mu\text{g/g}$ ; Figure 2,  $r^2 = 0.71$ ,  $p = 0.000$ ). Statistical tests demonstrated agreement between predicted and actual flux (Table 2 in Supporting Information). The equation

$$\log(\text{normalized flux}) = 1.434 + [0.554 \times \log(\text{Hg substrate})] \quad (2)$$

was used in the modeling to convert substrate concentration to an estimated average daily flux. This equation was used to predict the average daily emission from substrate of known Hg concentration. For example, a  $1 \text{ km}^2$  area having  $10 \mu\text{g/g}$  Hg in substrate would produce an estimated average daily flux of  $97.2 \pm 37 \text{ ng m}^{-2} \text{ h}^{-1}$  or  $2.3 \text{ g}$  of Hg during a sunny day. The uncertainty reported with flux estimates is the 95% confidence interval derived from the regression curve of eq 2.

**GIS Modeling.** The data were manipulated using ARC/INFO 8.0 and ArcView 3.2 with the Spatial Analyst 2.0 extension. The Nevada grids consist of approximately 35 328 000 cells (90 m cell size), projected into UTM zone 11, NAD27. The GIS used for the modeling comprise five primary layers: (i) a geologic layer consisting of 1:250 000 scale geologic maps, (ii) an alteration layer containing polygons derived from LANDSAT 7 images emphasizing clays and iron oxides indicative of hydrothermal alteration, (iii) a layer consisting of point Hg flux values derived from rock and soil Hg concentrations, using eq 2, (iv) a meteorological layer used to adjust Hg flux as a function of sunlight and cloud cover, and (v) a layer removing the effects of wet and dry Hg deposition, using data from the Mercury Deposition Network (MDN) (25).

**TABLE 1. Data from Geologic Map Layer Showing Sample Density, Cutoff Value, Mean of Unenriched "Background" Population, and Assigned Hg Flux for Each Geologic Unit**

no.	geologic unit	area (km <sup>2</sup> )	no. of samples	samples (per km <sup>2</sup> )	cutoff value enriched/background populations (μG/G)	samples less than cutoff (background)	mean of background population (μG/G)	Hg flux (ng m <sup>-2</sup> h <sup>-1</sup> )
1	Quaternary alluvium	118 131	8 504	0.07	0.08	4 369	0.028	3.7
2	Quaternary playa & lake deposits	12 543	164	0.01	0.16	95	0.049	5.1
3	Quaternary colluvium/older alluvium	8 868	949	0.11	0.12	546	0.047	5.0
4	Quaternary basalt	2 442	233	0.10	0.07	66	0.031	3.9
5	Quaternary hot spring deposits	14	2	0.14	none		2.560	45.7
6	Quaternary sedimentary rocks	1 370	69	0.05	0.10	31	0.047	5.0
7	Tertiary ashflow tuffs	37 746	10 249	0.27	0.11	4 846	0.042	4.7
8	Tertiary mafic volcanic rocks	18 867	4 690	0.25	0.14	2 449	0.050	5.2
9	Tertiary felsic volcanic rocks	8 144	3 874	0.48	0.11	1 543	0.053	5.3
10	Tertiary felsic intrusive rocks	292	203	0.70	0.13	132	0.065	6.0
11	Tertiary granitic rocks	385	358	0.93	0.10	278	0.031	4.0
12	Tertiary volcaniclastic rocks	14 834	2 029	0.14	0.08	893	0.032	4.1
13	Tertiary sedimentary rocks	7 180	1 018	0.14	0.10	457	0.039	4.5
14	Tertiary mafic intrusive rocks	681	178	0.26	0.10	110	0.024	3.4
15	Tertiary intermediate/mafic ashflows	1 104	381	0.35	0.12	166	0.057	5.5
16	Mesozoic granitic rocks	7 213	2 101	0.29	0.09	951	0.031	4.0
17	Mesozoic mafic intrusive rocks	298	345	1.16	0.07	123	0.029	3.8
18	Mesozoic metavolcanic rocks	1 643	1 253	0.76	0.13	679	0.054	5.4
19	Mesozoic limestone	1 090	2 331	2.14	0.12	714	0.058	5.6
20	Mesozoic sedimentary rocks	4 779	1 972	0.41	0.11	830	0.044	4.8
21	Mesozoic felsic volcanic rocks	257	118	0.46	0.10	32	0.048	5.1
22	Mesozoic metamorphic rocks	236	140	0.59	0.07	51	0.028	3.7
23	Paleozoic Golconda allocthon	1 461	4 620	3.16	0.09	1 802	0.038	4.4
24	Paleozoic Antler Sequence	1 783	2 799	1.57	0.10	1 458	0.030	3.9
25	Paleozoic Western Assemblage	4 697	9 190	1.96	0.10	5 352	0.032	4.1
26	Paleozoic limestone	19 208	10 099	0.53	0.09	5 215	0.035	4.2
27	Paleozoic shelf sedimentary rocks	6 432	2 822	0.44	0.09	1 223	0.036	4.3
28	Paleozoic metavolcanic rocks	408	292	0.72	0.08	95	0.039	4.5
29	Paleozoic metamorphic rocks	514	0	0.00	none	0		4.0
30	pre-Cambrian rocks, undifferentiated	2 368	745	0.31	0.07	346	0.028	3.8
31	altered/unknown rocks	77	99	1.28	none		3.960	58.2
32	water	1 132	0	0.00	none	0		0.00

**Geologic Layer.** The geologic map layer utilized 1:250 000 scale county geologic maps of Nevada digitized into ArcInfo coverages (26). Geologic units were reclassified into 32 standard geologic surface units, combined into one mosaic coverage, and converted to grid (Table 1). Mercury flux values were assigned to each geologic unit by spatially joining the geologic layer to the Hg concentration database. All samples in each geologic unit were separated into Hg subpopulations using cumulative frequency plots (Figure 2 in Supporting Information). The lowest concentration subpopulation was taken to be the nonenriched or "background" population. The break between nonenriched and enriched samples was taken as the first inflection point. The flux value assigned to each geologic unit was the mean Hg concentration of the background-value subpopulation. For the two geologic units associated with alteration (Quaternary hot springs and altered/unknown), the mean concentration for all samples was used. Water bodies were assigned a flux of zero.

The maximum Hg concentration for all 29 unaltered geologic units derived using this method ranged from 0.07 to 0.16 μg/g. The means of unaltered geologic units ranged from 0.024 to 0.065 mg/g (average 0.040 μg/g). These mean values were converted to Hg flux using eq 2 and became default flux values for the geologic units. These calculated means compare favorably with established mean Hg concentrations for unaltered rocks and soils (27).

**Alteration Layer.** The alteration layer was produced by digitizing polygons around altered areas visible from 1992/1993 LANDSAT 7 images of Nevada (Figure 1A). Band ratios were chosen that emphasize aspects of hydrothermal alteration (hydrothermal clay and iron oxide from weathered

sulfide minerals). Specifically, a band 5/band 7 = red, band 3/band 1 = green, and band 3/band 5 = blue ratioed image (28) was created after masking out vegetation and cloud cover. Care was taken not to include primary clay or iron oxides. To aid in distinguishing alteration, LANDSAT data were converted to Munsell coordinates, and alteration masks of clay and iron oxide hues were generated, utilizing a technique modified to work with Thematic Mapper data (29). Polygons representing active or recently active precious and base metal mines and active geothermal areas were also included in this layer.

Polygons in the alteration layer were used to separate areas of hydrothermal alteration from "fresh", unaltered geologic units. Areas inside alteration polygons were considered part of the naturally enriched Hg population, while outside areas were designated members of the background or nonenriched Hg population. Polygon edges were "hard boundaries", so that flux values associated with either population could not cross the boundary.

Areas within alteration polygons were assigned flux values. The alteration polygon layer was spatially joined to the sample database, so samples in alteration polygons could be categorized according to the percentage of samples having anomalous (>0.1 μg/g Hg; 30) mercury in substrate. Those polygons containing samples were divided into five categories (categories 1–5, Table 2). The Hg flux values assigned to categories 1 and 2 were the calculated flux using the arithmetic mean and the geometric mean of the samples, respectively. For categories 3–5, half the geometric mean was used because sampling in altered areas by exploration groups tends to focus on the most highly altered rocks, which

TABLE 2. Categories of Alteration Polygons from Alteration Layer

category	description of polygons	no. of polygons	samples in category	geom. mean samples ( $\mu\text{g/g}$ )	Hg concn used ( $\mu\text{g/g}$ )	flux ( $\text{ng m}^{-2} \text{h}^{-1}$ )
1	<5% samples in polygon anomalous	206	4 284	0.04 <sup>a</sup>	0.04	4.6
2	5–25% samples in polygon anomalous	88	3 588	0.04	0.04	4.9
3	25–75% samples in polygon anomalous	505	37 821	0.16	0.08	6.6
4	75–95% samples in polygon anomalous	379	6 270	0.73	0.36	15.5
5	>95% of samples in polygon anomalous	21	713	1.94	0.97	26.7
6	active hot springs having alteration	68	76	1.27	1.27	31.0
7	active/recently active metal mines	84	300	0.100	<i>b</i>	
8	polygons with historic Hg mines/prospects	9	0	none	0.15	9.5
9	polygons with historic mines/prospects	66	0	none	0.10	7.6
10	polygons with no samples or historic mines	593	0	none	0.08	6.7

<sup>a</sup> Arithmetic mean value. <sup>b</sup> See Table 3 in Supporting Information.

TABLE 3. Sample Types and Areas of Influence for Flux Layer

sublayer	sample types	representative	population	area of influence assigned to sample
1	rock chip and soils <0.1 $\mu\text{g/g}$ Hg outside alteration polygons	more	geologic units outside polygons	1000 m radius (3.14 $\text{km}^2$ )
2	rock chip and soils >0.1 $\mu\text{g/g}$ Hg, outside alteration polygons	less	geologic units outside polygons	100 m (0.03 $\text{km}^2$ )
3	rock chip and soils inside alteration polygons	more	inside alteration polygons	1000 m (3.14 $\text{km}^2$ )
4	mine dumps, prospect pits	less	both	100 m (0.03 $\text{km}^2$ )

would overestimate the actual mean of all potential samples within that polygon.

Some alteration polygons lacked sample data. For these polygons, flux values were assigned using historic mine and prospect data (Table 2; 3I). Polygons without sample or historic data were assigned a flux of  $6.7 \text{ ng m}^{-2} \text{ h}^{-1}$ , equivalent to a high background ( $0.08 \mu\text{g/g}$ ) substrate concentration.

Active hot spring alteration formed another polygon category. Only active hot springs with visible alteration were assigned a polygon. The geometric mean Hg concentration of all substrate samples within these polygons ( $1.27 \mu\text{g/g}$ ) was converted to flux, and a corresponding value of  $31.0 \text{ ng m}^{-2} \text{ h}^{-1}$  was assigned to these polygons.

Active or recently active precious and base metal mines constituted a final category of alteration polygons. The mine polygons represent the total area from open pits, dumps, stockpiles, and leach pads in 1992/1993 when the LANDSAT photographs were taken. Average Hg substrate values from mines were used (Table 3 in Supporting Information).

**Flux Layer.** The flux layer consisted of the 71 227 substrate samples whose Hg concentration was converted to average daily flux using eq 2. This layer was subdivided into four sublayers based on sample type, Hg concentration, and alteration (Table 3). These subdivisions simulate natural sample populations and provided a basis for assigning areas of influence to each of the sample points.

The first sublayer was composed of rock and soil samples in geologic units outside alteration polygons with Hg concentrations below  $0.1 \mu\text{g/g}$  (e.g., nonenriched). Samples of this category were considered representative of the background population and were assigned a 1000 m radius of influence ( $3.14 \text{ km}^2$  area). Enriched rock chip and soil samples ( $>0.1 \mu\text{g/g}$  Hg) in geologic units outside alteration zones constituted the next layer and were deemed representative of only small areas (e.g., quartz veins, jasperoid, and alteration too small to be visible using LANDSAT imagery). These samples were given a 100 m radius of influence ( $0.03 \text{ km}^2$  area). Enriched and nonenriched rock chip and soil samples inside alteration polygons made up the third sublayer. Since hydrothermally altered zones commonly contain elevated Hg concentrations, all samples

of this category were considered representative and assigned a 1000 m radius of influence ( $3.14 \text{ km}^2$  area). The last sublayer was composed of mine dump and prospect pit samples both inside and outside of alteration polygons: these samples were considered only representative of small areas of enhanced alteration and were assigned a 100 m radius of influence ( $0.03 \text{ km}^2$  area; Table 3).

An inverse-distance weighting interpolation method (power = 2, neighbors = 12) was used to convert sample values (zero-dimensional points) onto a sublayer (two-dimensional area). Each sublayer was interpolated separately so as to avoid exposure from other sample populations. Sample areas were created by buffering the appropriate size from sample points and clipping these areas from the interpolation grids.

**Composite Hg Flux Layer.** The geologic, alteration, and flux layers were combined to form a single composite Hg flux layer. This layer consisted of flux values from the geologic layer with the areas corresponding to alteration polygons removed and replaced by flux values from the alteration layer. From this layer, sample areas from the four sample sublayers were removed and replaced with the interpolated sample values. The average daily flux calculated for Nevada from this step is  $5.0 \pm 1.6 \text{ ng m}^{-2} \text{ h}^{-1}$  (Table 4 and Figure 3A in Supporting Information) and represents gross Hg flux under completely sunny conditions.

**Meteorological Layer.** Because mercury flux is strongly affected by exposure to sunlight (23, 32, 33), a meteorological layer was added to the GIS to adjust flux values for periodic cloudy conditions. To accomplish this, successive flux measurements taken from the same location during intermittent sun and cloud conditions were used to derive

$$\log(C) = [\log(S) \times 1.034] - 0.536 \quad R^2 = 0.99, P = 0.005 \quad (3)$$

where  $C$  is the measured flux under cloudy conditions, and  $S$  is the flux derived during sunlight conditions (cloudless with solar radiation  $>620 \text{ w/m}^2$ ). This equation was applied to a contoured map of annual average percent sunshine for the region (34; Figure 4 in Supporting Information)

TABLE 4. Estimated Hg Fluxes from Nevada, Calculated from the Model<sup>a</sup>

name	mean flux (ng m <sup>-2</sup> h <sup>-1</sup> )	total area (km <sup>2</sup> )	hourly flux (g)	daily flux (kg)	yearly emission (kg)	total flux (% of ADF)
NV flux before meteorological adjustment	5.0 ± 1.6	286 187	1 440	34.5	12 600	
NV flux after meteorological adjustment	4.2 ± 1.4	285 043	1 190	28.6	10 400	100
area outside polygons after meteorological adjustment	3.5 ± 1.2	265 043	934	22.4	8 180	78
alteration polygons after meteorological adjustment	12.9 ± 3.6	20 001	257	6.2	2 250	22
hot spring polygons after meteorological adjustment	70.6 ± 25.0	86	6.1	0.1	53	0
flux from all mines after meteorological adjustment	61.8 ± 21.3	251	15.6	0.4	136	1
porphyry copper mines after meteorological adjustment	4.5 ± 1.5	25	0.1	0.0	1	0
adjusted NV flux, 1:1 wet-dry deposition, 100% reemitted	2.8	285 038	785	18.8	6 870	66
adjusted NV flux, 1:1 wet-dry deposition, 50% reemitted	3.5	285 038	988	23.7	8 650	83
adjusted NV flux, 1:1 wet-dry deposition, 30% reemitted	3.7	285 038	1 070	25.7	9 370	90
adjusted NV flux, 1:2 wet-dry deposition, 100% reemitted	2.0	285 038	583	14.0	5 110	49
adjusted NV flux, 1:2 wet-dry deposition, 50% reemitted	3.1	285 038	886	21.3	7 760	75
adjusted NV flux, 1:2 wet-dry deposition, 30% reemitted	3.5	285 038	1 000	24.0	8 760	84

<sup>a</sup> Alteration polygons (alteration, mines, hot springs) comprise approximately 7% of Nevada; the remainder is considered unaltered. Uncertainty in flux estimates is 95% confidence interval from regression of eq 2 (Figure 2). Uncertainty in wet-dry deposition was not estimated.

and entered into the GIS using

$$A = (S\%/100 \times S) + [\{\exp^{10}([\log(S)] \times 1.034 - 0.536)\} \times (1 - (S\%/100))] \quad (4)$$

where *A* is flux adjusted to partial cloudy conditions, *S%* is the average daily sunshine percentage, and *S* is the Hg flux under sunny conditions. This equation adjusts the gross Hg flux to one reflecting annual cloudy conditions. The average daily flux adjusted for cloudy conditions (ADF) for Nevada is 4.2 ± 1.4 ng m<sup>-2</sup> h<sup>-1</sup> (Figure 3B in Supporting Information).

**Adjustment for Deposition and Re-emission.** Mercury is deposited onto substrate throughout the globe in the form of wet and dry deposition (3, 16). Our data set of 303 in situ measurements included 44 negative fluxes indicative of net Hg deposition. These negative flux measurements were not used in the modeling, so the ADF of 4.2 ng m<sup>-2</sup> h<sup>-1</sup> includes Hg re-emitted after atmospheric deposition. Although current modeling and measurements of wet and dry Hg deposition involve significant uncertainty, we modeled Hg deposition in an attempt to subtract out this re-emitted component. The remaining flux would yield an estimate of new or “geologic” mercury entering the atmospheric pool.

Mercury deposition was modeled assuming that Nevada precipitation is a function of elevation, which in turn influences Hg deposition (35). A weighted average of annual deposition rates from the MDN was applied to a digital elevation model (DEM) of Nevada. Although no MDN sites are currently operating in Nevada, sites in Caballo, NM, and Buffalo Pass, CO, provide a reasonable estimate of wet Hg deposition for intermediate- and high-elevation areas in Nevada. Dry deposition rates are thought to be similar to wet deposition (36, 37), and multiple model scenarios were run using different wet:dry ratios and re-emission rates (Table 4). The estimated wet + dry deposition value was subtracted from each cell of the ADF grid. Recent re-emission rates determined using stable Hg isotopes suggest that 10–30% of deposited Hg is re-emitted (38). Using a 1:2 wet:dry ratio and 30% re-emission rate, 0.7 ng/m<sup>2</sup>h (17%) of the ADF is previously deposited and reemitted Hg, while 3.5 ng/m<sup>2</sup>h (24 kg/day) is new geologic Hg entering the global atmospheric pool (Figure 3C in Supporting Information). Because the uncertainty involved in this step of the modeling is difficult to quantify, being based on extrapolation of data to Nevada from areas outside the state, most conclusions below do not include the re-emission term.

## Results and Discussion

The results of this modeling are tabulated in Table 4, on the basis of a day having 12 h of sunshine and moderate

temperatures. Under ideal sunny conditions, Nevada substrate would emit 5.0 ± 1.6 ng m<sup>-2</sup> h<sup>-1</sup> or 34.5 kg of Hg/day. Given average cloudy conditions (after the meteorological adjustment), emissions would decrease 17% to an ADF of 4.2 ± 1.4 ng m<sup>-2</sup> h<sup>-1</sup> (28.6 kg/day). This value is over three times that of earlier estimates (3). On the basis of average flux values having been adjusted for meteorological conditions, the majority of the mercury (78% or 22.4 kg/day) is emitted from substrate outside hydrothermal alteration zones, predominantly from unaltered rocks having very low concentrations exposed over very large areas. Enriched rocks outside alteration polygons (sublayer 2, Table 3) do not contribute substantially to this value. The ADF outside alteration polygons (3.5 ± 1.2 ng m<sup>-2</sup> h<sup>-1</sup>) compares well with other flux measurements from nonenriched substrate (6, 16). Zones of alteration in Nevada, which comprise 7% of the area, emit approximately 22% of the Hg, yielding approximately 6.2 kg of Hg/day in the atmosphere. The ADF of 12.9 ± 3.6 ng m<sup>-2</sup> h<sup>-1</sup> includes highly enriched as well as unenriched substrate within alteration polygons.

Substrate within active and recently active metal mines constitute ~0.1% of the area of Nevada yet produce approximately 1% of the total natural Hg flux (0.4 kg/day). These mines are located predominantly within hydrothermal alteration zones. Although the ADF from substrate in mines is higher (61.8 ± 21.3 ng m<sup>-2</sup> h<sup>-1</sup>) than the average of alteration zones, the amount of Hg given off by alteration zones (without mines) is 17 times as great. The subset of porphyry copper mines in the state has low Hg flux values (4.5 ± 1.5 ng m<sup>-2</sup> h<sup>-1</sup>) and produces negligible amounts of Hg (~3 g/day) as compared with other sources.

The hydrothermal alteration around active geothermal areas yielded the highest ADF values (70.6 ± 25.0 ng m<sup>-2</sup> h<sup>-1</sup>) although their total area (86 km<sup>2</sup>) is small. Their contribution to the atmospheric pool is 0.1 kg/day or 0.5% of the Nevada total. This value does not include direct contributions from the active geothermal system.

One consequence of the effect of cloudiness on Hg flux is that substrate with the same Hg concentration in different parts of Nevada will emit Hg to the atmosphere at different rates. For example, a patch of soil with 10 μg/g Hg in Wells, NV (65% average sunshine), will emit an ADF of 75 ng m<sup>-2</sup> h<sup>-1</sup>. The same soil, if located in Las Vegas (84% average sunshine) would emit an ADF of 87 ng m<sup>-2</sup> h<sup>-1</sup>, a 16% increase. Thus average sunshine might be a contributing factor in deciding remediation strategies.

Assuming the range of wet + dry Hg deposition and re-emission rates in Table 4, the model indicates geologic Hg constitutes between 49% and 90% of the ADF (2.0–3.7 ng

**TABLE 5. Comparison of Hg Emissions from Nevada Substrate with Estimates from Selected Anthropogenic Sources in the United States**

emission source	Hg emissions (Mg/yr)	ref
substrate in Nevada	10.4	this study
substrate in Nevada (estimate)	2.8	3
U.S. coal-fired utility plants	46.9	39
U.S. municipal waste combustors	26.9	39
U.S. medical waste incinerators	14.6	39
U.S. chlor-alkali plants	6.5	39
U.S. Portland cement manufacturers	4.4	39
U.S. pulp and paper mills	1.7	39

$\text{m}^{-2} \text{h}^{-1}$ ) being emitted from Nevada (Table 4). If so, the net daily flux of geologic Hg to the atmosphere from Nevada is  $2.0\text{--}3.7 \text{ ng m}^{-2} \text{ h}^{-1}$  ( $14.0\text{--}25.7 \text{ kg/day}$ ), 2–3 three times that predicted for areas within Hg belts (3).

Little research has been done to quantify the relationship between seasonal and episodic effects such as snow cover, precipitation, and vegetation to Hg flux. This model does not account for these factors. If modeling an “average day” at/near the equinox can be extrapolated to an annual rate, substrate in Nevada fluxes 10 400 kg of Hg to the atmosphere each year, of which approximately 5100–9100 kg is new geologic Hg entering the global atmospheric pool.

Table 5 compares Hg emissions calculated in this study with emission estimates from several anthropogenic sources in the United States (39). Even with uncertainty associated with the model and neglecting the effects of seasonal and episodic factors, natural Hg emissions from Nevada are probably of similar magnitude as these anthropogenic emissions. However, Nevada Hg emissions should not be considered representative of well-vegetated areas within global Hg belts due to the profound effects of shading.

**Comparison with Other Models.** Two studies (5, 24) used GIS to estimate Hg flux from mining districts in Nevada using identical sampling equipment and protocols. Since both these estimates utilize in situ flux measurements, the opportunity existed for comparison with this substrate-based model. One study (5) using 29 in situ Hg flux measurements from geologic units in and adjacent to the Ivanhoe (mercury) mining district, NV, estimated an average Hg flux of  $17.5 \text{ ng m}^{-2} \text{ h}^{-1}$  for the  $586 \text{ km}^2$  area. Their model made no adjustments for meteorological conditions. Using the same study area, we calculated an ADF of  $13.8 \text{ ng m}^{-2} \text{ h}^{-1}$  or  $17.4 \text{ ng m}^{-2} \text{ h}^{-1}$  without the meteorological adjustment.

Similarly, scaling estimates for two other mining districts in Nevada are available: the Peavine District northwest of Reno and the Flowery Peak area southeast of Reno (24). All data reported are without the meteorological adjustment. At the Peavine study site ( $121 \text{ km}^2$ ), 17 flux measurements were used to calculate an average emission of  $10.0 \text{ ng m}^{-2} \text{ h}^{-1}$  Hg. Our study estimated a similar value of  $9.7 \text{ ng m}^{-2} \text{ h}^{-1}$ . At the Flowery Peak study area ( $252 \text{ km}^2$ ) 17 flux and substrate samples were used to calculate an average daily Hg flux of  $18.5 \text{ ng m}^{-2} \text{ h}^{-1}$ . Our modeling yielded a significantly lower flux estimate of  $6.3 \text{ ng m}^{-2} \text{ h}^{-1}$ . Two factors appear to explain the discrepancy. First, substrate samples were unavailable in our database for a highly Hg-enriched area sampled in ref 5, so that lower default values were used. Second, one location in the study area consistently yields higher flux values ( $70\text{--}80 \text{ ng m}^{-2} \text{ h}^{-1}$  noontime) than predicted by substrate concentration ( $0.03 \mu\text{g/g}$ ), which suggests a Hg contribution from depth that our model cannot predict. These comparisons indicate that the model is conservative but accurately predicts flux emissions from substrate at the regional scale when a sufficient substrate sample density is reached.

## Acknowledgments

We thank the Kennecott Exploration Company, Kinross Gold Corporation, Gary Raines (U.S. Geological Survey), Russell Bullock (NOAA), the Nevada Bureau of Mines and Geology, Phelps Dodge Corporation, and the UNR DeLaMare Library and Keck Center for their help in providing data and/or technical support for this project. UNR graduate students Mark Coolbaugh, Mark Engle, David Nacht, Brian Fitzgerald, and Chris Sladek contributed field observations. Three anonymous reviewers considerably helped the manuscript. This project was funded through EPA Star Grant EPA-R827634-01-1 and a grant from EPRI.

## Supporting Information Available

Additional tables, figures, and references. This material is available free of charge via the Internet at <http://pubs.acs.org>.

## Literature Cited

- Rasmussen, P. E.; Edwards, G. C.; Kemp, J. R.; Fitzgerald-Hubble, C. R.; Schroeder, W. H. In *Proceedings on the Metals in the Environment: An International Symposium*; Skeaff, J., Ed.; 1998; pp 74–82.
- Gustin, M. S.; Coolbaugh, M.; Engle, M.; Fitzgerald, B.; Keislar, R.; Lindberg, S. E.; Nacht, D.; Quashnick J.; Rytuba, J.; Sladek, C.; Zhang H.; Zehner, R. *Environ. Geol.* (in press).
- Lindqvist, O.; Johansson, K.; Aastrup, M.; Anderson, A.; Bringmark, L.; Hovsenius, G.; Iverfeldt, A.; Meili, M.; Timm, B. *Water, Air, Soil Pollut.* **1991**, *55*, 1–261.
- Zehner, R. E.; Gustin, M. S. *Assessing and Managing Mercury from Historic and Current Mining Activities*, Symposium Volume; San Francisco; 2000; pp 135–140.
- Engle, M. A.; Gustin, M. S.; Zhang, H. *Atmos. Environ.* **2001**, *35*, 3987–3997.
- Zhang, H.; Lindberg, S. E.; Marsik, F. J.; Keeler, G. J. *Water, Air, Soil Pollut.* **2000**, *90*, 1–19.
- Benesch, J. A.; Gustin, M. S.; Schorran, D. E.; Coleman, J.; Johnson, D. A.; Lindberg, S. E. Presented at the 6th International Conference on Mercury as a Global Pollutant, Minamata, Japan, 2001; AT-39.
- Gustin, M. S.; Lindberg, S.; Marsik, F.; Casimir, A.; Ebinghaus, R.; Edwards, G.; Hubble-Fitzgerald, C.; Kemo, R.; Kock, H.; Leonard, T.; London, J.; Majewski, M.; Montecinos, C.; Owens, J.; Pilote, M.; Poissant, L.; Rasmussen, P.; Schaedlich, F.; Schneeberger, D.; Schroeder, W.; Sommar, J.; Turner, R.; Vette, A.; Wallschlaeger, D.; Xiao, Z.; Zhang, H. *J. Geophys. Res.* **1999**, *104* (D17), 21,831–21,844.
- Friedli, H. R.; Radke, L. F.; Lu, J. Y. *Geophys. Res. Lett.* **2001**, *28*, 3223–3226.
- McCarthy, J. H.; Vaughn, W. W.; Learned, R. E.; Meuschke, J. L. *Geol. Sur. Cir. (U.S.)* **1969**, *609*, 1–15.
- Maciolek, J.; Jones, V. T. In *Bulk Mineable Precious Metal Deposits of the Western United States: Symposium Proceedings*; Shafer, R. W., Cooper, J. J., Vikre, P. G., Eds.; Geological Society of Nevada: Carson, 1988; p 746.
- Goff, F. *Assessing and Managing Mercury from Historic and Current Mining Activities*, Symposium Volume; San Francisco, CA, 2000; pp 209–213.
- Ellis, A. J. *Geothermics* **1977**, *6*, 175–182.
- Robertson, D. E.; Crecelius, E. A.; Fruchter, J. S.; Ludwick, J. D. *Science* **1977**, *196*, 1094–1097.
- Ferrera, R.; Mazzolai, B.; Edner, H.; Svanberg, S.; Wallinder, E. *Sci. Total Environ.* **1998**, *213*, 13–23.
- Schroeder, W. H.; Munthe, J. *Atmos. Environ.* **1998**, *32*, 5, 809–822.
- Gustin, M. S.; Rasmussen, P.; Edwards, G.; Schroeder, W.; Kemp, J. *J. Geophys. Res.* **1999**, *104* (D17), 21,873–21,878.
- Thorton, C. H.; Ketner, K. B.; Brooks, W. E.; Snee, L. W.; Zimmerman, R. A. *Geology and Ore Deposits of the Great Basin, Symposium Proceedings*; Raines, G. L., Lisle, R. E., Schafer, R. W., Wilkinson, W. H., Eds.; Geological Society of Nevada: Carson, 1991; Vol. 1, pp 25–45.
- Garside, L. J. *Nev. Bur. Mines Geol. Open-File Rep.* **1994**, No. OF94-2, 1–108.
- Rytuba, J. J.; Heropoulos, C. *U.S. Geol. Sur. Bull.* **1992**, 1877.
- Baedecker, P. A.; Grossman, J. N.; Buttleman, K. P. *U.S. Geol. Sur. Digital Data Ser.* **1998**, No. DDS-47 (CD-ROM).
- Tingley, J. V. *Nev. Bur. Mines Geol. Open-File Rep.* **1998**, No. 98-8, (CD-ROM).

- (23) Gustin, M. S.; Biester, H.; Kim, C. S. *Atmos. Environ.* (in press).
- (24) Engle, M. A.; Gustin, M. S. *Sci. Total Environ.* **2002**, *290*, 91–104.
- (25) Mercury Deposition Network. National Atmospheric Deposition Program. <http://nadp.sws.uiuc.edu/mdn/> (accessed January 2001).
- (26) Hess, R. H.; Johnson, G. *Nev. Bur. Mines Geol. Open-File Rep.* **1997**, No. 97-1 (CD-ROM).
- (27) U.S. Geological Survey. *U.S. Geol. Sur. Prof. Pap.* **1970**, No. 713, 1–67.
- (28) Sabins, F. F. *Remote Sensing: Principles and Interpretation*, 2nd ed.; W. H. Freeman and Co.: New York, 1987; 449 pp.
- (29) Raines, G. L. *Proceedings, Eleventh International Symposium on Remote Sensing of the Environment*; 1977, 1463–1472.
- (30) Gustin, M. S.; Lindberg, S. E.; Austin, K.; Coolbaugh, M.; Vette, A.; Zhang, H. *Sci. Total Environ.* **2000**, *259*, 61–72.
- (31) Mason, G. T., Jr.; Arndt, R. E.; Buttleman, K. *U.S. Geol. Sur. Digital Data Ser.* **1996**, No. DDS-20 (CD-ROM).
- (32) Carpi, A.; Lindberg, S. E. *Atmos. Environ.* **1998**, *32*, 873–882.
- (33) Zhang, H.; Lindberg, S. E.; Barnett, M. O.; Vette, A. F.; Gustin, M. S. *Atmos. Environ.* **2002**, *36*, 835–846.
- (34) Western Regional Climate Center, Desert Research Institute. <http://www.wrcc.dri.edu/summary/lcd.html> (accessed September 2000).
- (35) Bullock, Russell O. NOAA Air Resources Laboratory, NC, personal communication, 2001.
- (36) Hoyer, M.; Burke, J.; Keeler, G. *Water, Air, Soil Pollut.* **1995**, *80*, 199–208.
- (37) Lindberg, S. E.; Turner, R. R.; Meyers, T. P.; Taylor, G. E., Jr.; Schroeder, W. H. *Water, Air, Soil Pollut.* **1991**, *56*, 577–594.
- (38) Lindberg, S.; Dong, W.; Kuiken, T.; Hintelmann, H.; St. Louis, V. Presented at 6th ICMGP Conference, Minamata, Japan, October 2001.
- (39) U.S. Environmental Protection Agency, Office of Air Quality Planning Standards and Office of Research and Development; *Mercury Study Report to Congress*; U.S. Government Printing Office: Washington, DC, 1997; EPA-452/R-97-004.

*Received for review September 28, 2001. Accepted July 16, 2002.*

ES015723C